Spectral Properties of Photocurrent Fluctuations in Avalanche Photodiodes

Gokalp Kahraman, *Student Member, IEEE,* Bahaa E. A. Saleh, *Fellow Member, IEEE,* and Malvin C. Teich, *Fellow Member, IEEE*

Abstract— **We provide a stochastic model that describes the time dynamics of double-carrier multiplication in an avalanche photodiode (APD) and obtain the autocorrelation function and the spectral characteristics of the photoelectric current. The photoelectric pulse generated by an APD as a result of a single injected photoelectron is regarded as a nonstationary random function of time (the impulse response function). A discrete stochastic model for the electron/hole motion and multiplication is defined on a spatio-temporal lattice and used to derive recursive equations for the mean, the variance, and the autocorrelation of the impulse response as functions of time. Correlation properties of the impulse response are studied for a conventional and a multilayer (superlattice) APD with the same mean gain and carrier-ionization rate ratio. The power spectral density of the photocurrent in response to a Poisson-distributed stream of photons of uniform rate is evaluated.**

I. Introduction

STUDIES of the statistical properties of the response of avalanche photodiodes have largely focused on the gain statistics without incorporating the time dependence of the avalanching process itself [1]–[22]. Explicit formulas for the gain and the excess noise factor have been already derived for both conventional and superlattice devices [1]–[8]. Although the excess noise factor is a useful statistic representing the lowest order statistical properties of the gain fluctuations, it does not provide the complete statistical description of the impulse response stochastic process.

The performance analysis of a digital optical transmission system requires knowledge of the temporal statistics of the impulse response function. Since APD's with double-carrier multiplication properties are vital components of fiber-optic communication systems, accurate evaluation of their noise is necessary. Knowledge of the autocorrelation function of the impulse response makes this evaluation possible [23]–[26].

Studies of the temporal dynamics of the avalanching process were limited to the mean impulse response and its Fourier transform [27]–[37]. Naqvi [38] provided an expression for the mean square avalanche current by including a frequency dependent factor in McIntyre's [1] mean square gain expression. He solved transport equations for the mean current densities assuming stationarity of the multiplication process, i.e., that the transient (nonstationary) contribution is negligible at high gains. However, in high-data-rate optical transmission systems the transient contribution is clearly important. Walma and Hackam [39] provided a partial solution of the problem by considering only the arrival of electrons at the edge of the device. They did not determine the photocurrent response. The autocorrelation function of the impulse response was first determined by Matsuo *et al.* [30] and later by Hayat *et al.* [31] for single-carrier multiplication APD's including the dead-space effects.

In this paper we derive the autocorrelation function of the impulse response of a double-carrier multiplication APD assuming general conditions including nonuniform carrier ionization rates and unequal carrier velocities. A discrete stochastic model is first determined to describe the APD multiplication process, then recursive equations for the mean, variance and autocorrelation of the impulse response are derived and evaluated. The theory is applied to a conventional APD (CAPD) and a multiquantum well (MQW) APD with the same gain and carrier-ionization rate ratio. The CAPD was found to have more correlated response, a higher excess noise factor, and a slower response. However, the signal-to-noise ratio of the current response is greater than the MQW-APD. For both devices, the standard deviation of the current (which represents noise) is low at the onset of multiplication, sharply peaks at about the same time but does not die off as rapidly as the mean current. For a high-data-rate optical communication system, this type of noise will increase intersymbol interference and therefore reduce the bit-error-rate. Finally, we computed the mean, the variance, and the autocovariance function of the photoelectric current due to a uniform stream of Poisson distributed photons corresponding to a constant optical power. The photocurrent generated in the conventional APD has a narrower power spectral density but a higher signal-to-noise ratio than that of the superlattice APD.

II. The Stochastic Model

A. Impulse Response

We consider an APD with a multiplication region of width W. The electron and hole ionization rates are $\alpha(x)$ and $\beta(x)$, and their saturation velocities are v_e and v_h, respectively. Assuming a single-electron injected at $x = 0$ at $t = 0$ into the multiplication region $x \in [0, W]$, typical trajectories for the carriers generated by ionizations are depicted in the space-time diagram in Fig. 1. The initial injected electron drifts under the strong electric field in the multiplication region, and generates

Manuscript received July 15, 1991. This work was supported by the National Science Foundation.

G. Kahraman and B. E. A. Saleh are with the Department of Electrical and Computer Engineering, University of Wisconsin, Madison, WI 53706–1691.

M. C. Teich is with the Center for Telecommunications Research, Department of Electrical Engineering, Columbia University, New York, NY 10027.

IEEE Log Number 9105884.

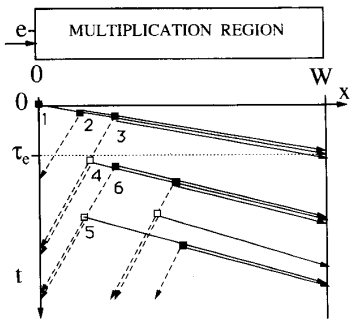

Fig. 1. Space-time diagram illustrating typical trajectories for the electrons and holes generated by ionizations as a result of an injected photoelectron at 1. The initial injected electron drifts along the solid line with saturation velocity v_e (the slope of the solid lines). It generates new electron-hole pairs at 2 and 3 by impact ionization. The holes travel in the opposite direction along the dashed lines with saturation velocity v_h, and can also generate new electron-hole pairs, for example at 4 and 5. The resulting carriers can themselves cause impact ionizations, for example at 6.

new electron-hole pairs by impact ionization. The holes travel in the opposite direction, and can also generate new electron-hole pairs. The resulting carriers can themselves cause impact ionizations, and so on. The process terminates when the last carrier leaves the multiplication region. The moving charges induce an electrical current in the external circuit, statistics of which we wish to determine.

Discretization: It is convenient to describe the motion of the carriers on a discrete space-time grid as shown in Fig. 2. The space-time coordinates x and t are replaced with discrete variables k and n, respectively. The ionization rates $\alpha(x)$ and $\beta(x)$ are transformed into discrete parameters $P[k]$ and $Q[k]$, representing the probability of electron and hole ionizations at each cell, respectively. If $Z[k,n]$ and $Y[k,n]$ are the number of electrons and holes at location k and time n, respectively, then the electric current induced by the motion of these carriers is

$$h[n] = \frac{q}{W}\sum_{k=1}^{L}\{v_e Z[k,n] + v_h Y[k,n]\} \tag{1}$$

where L is the number of spatial cells, and q is the magnitude of the electron charge. The gain of the APD is the area under the electric current divided by q

$$G = \frac{\Delta t}{q}\sum_{n=0}^{\infty} h[n] \tag{2}$$

where Δt is the time increment. The mean, autocorrelation function, and variance of the current $h[n]$ are respectively,

$$m_h[n] = \frac{q}{W}\sum_{k=1}^{L}\{v_e m_Z[k,n] + v_h m_Y[k,n]\} \tag{3}$$

$$\begin{aligned} R_{hh}[n,m] = \frac{q^2}{W^2}\sum_{k=1}^{L}\sum_{j=1}^{L}\{&v_e^2 R_{ZZ}[k,j;n,m] \\ &+ v_h^2 R_{YY}[k,j;n,m] \\ &+ 2v_e v_h R_{ZY}[k,j;n,m]\} \end{aligned} \tag{4}$$

$$\sigma_h^2[n] = R_{hh}[n,n] - m_h^2[n] \tag{5}$$

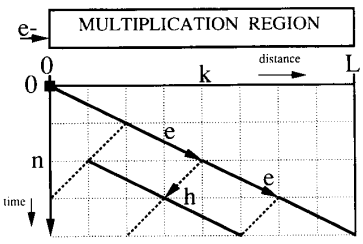

Fig. 2. Space-time grid showing the discrete motion of electrons and holes. Time and distance are represented by n and k, respectively. k_e and k_h are chosen such that $\frac{v_e}{v_h} \approx \frac{k_e}{k_h}$. In this diagram $\frac{k_e}{k_h} = 2$.

where

$$\begin{aligned} m_h[n] &= E\{h[n]\} \\ m_Z[k,n] &= E\{Z[k,n]\} \\ m_Y[k,n] &= E\{Y[k,n]\} \\ R_{hh}[n,m] &= E\{h[n]h[m]\} \\ R_{ZZ}[k,j;n,m] &= E\{Z[k,n]Z[j,m]\} \\ R_{YY}[k,j;n,m] &= E\{Y[k,n]Y[j,m]\} \\ R_{ZY}[k,j;n,m] &= E\{Z[k,n]Y[j,m]\}. \end{aligned}$$

The first and second moments of the APD gain are related to the statistics of $h[n]$ by

$$M = \frac{\Delta t}{q}\sum_{n=0}^{\infty} m_h[n] \tag{6}$$

and

$$M_2 = \frac{\Delta t^2}{q^2}\sum_{n=0}^{\infty}\sum_{m=0}^{\infty} R_{hh}[n,m]. \tag{7}$$

The spatio-temporal dynamics of the stochastic processes $Z[k,n]$ and $Y[k,n]$ are governed by the multiplication process and are controlled by the ionization probabilities $P[k]$ and $Q[k]$. Our goal is to determine the statistics of $Z[k,n]$ and $Y[k,n]$ so that the statistics of $h[n]$ can be derived from (1). The dynamics of the multiplication process is described in Section II-B, and recursive relations are derived for the moments of $Z[k,n]$ and $Y[k,n]$ in Section III. The mean, the variance, and the autocorrelation function of the impulse response are determined in Sections III-A, B, and C, respectively.

B. Dynamics of The Multiplication Process

Since the velocities of electrons and holes are different, an increment of time Δt corresponds to different electron and hole displacements $v_e\Delta t$ and $v_h\Delta t$, respectively. If the spactial cell size is selected to be $\Delta x = v_h\Delta t$, the electron displacement $v_e\Delta t$ will not necessarily be an integer multiple of Δx. We therefore choose two different integers k_e and k_h as the smallest integers satisfying $\frac{v_e}{v_h} \approx \frac{k_e}{k_h}$, so that in each time increment Δt, electrons will advance by $k_e\Delta x = v_e\Delta t$ and holes by $k_h\Delta x = v_h\Delta t$, where $\Delta x = \frac{W}{L}$. For example, if electrons are twice as fast as holes, then $k_e = 2$, and $k_h = 1$.

The dynamics of the electron and hole multiplication can then be modeled by the following equations:

$$Z[k,n] = Z[k-k_e,n-1] + z[k-k_e,n-1] + y[k+k_h,n-1] \quad (8a)$$

$$Y[k,n] = Y[k+k_h,n-1] + z[k-k_e,n-1] + y[k+k_h,n-1] \quad (8b)$$

for $k = 1,\cdots,L$ and $n = 0,\cdots,\infty$, where $z[k,n]$ and $y[k,n]$ represent the contribution of ionizations to the number of carriers. These contributions are governed by the cumulative number of carriers in the neighboring cells at earlier time increments in accordance with a Bernoulli probability law

$$z[k-k_e,n-1] = \sum_{i=1}^{Z[k-k_e,n-1]} a_i \quad (8c)$$

and

$$y[k+k_h,n-1] = \sum_{i=1}^{Y[k+k_h,n-1]} b_i \quad (8d)$$

where a_i and b_i are independent, and identically distributed Bernoulli random variables with probabilities $P[k]$ and $Q[k]$, respectively. Conditioned on $Z[k,n]$ and $Y[k,n]$, $z[k,n]$ and $y[k,n]$ are independent Binomial random variables with populations $Z[k,n]$ and $Y[k,n]$ and probabilities $P[k+k_e]$ and $Q[k-k_h]$, respectively. The initial condition is $Z[k,0] = \delta[k-1]$ and $Y[k,0] = 0$ for all k. The boundary conditions are: $Z[k,n] = Y[k,n] = 0$ for $k \notin [1,L]$ and $n > 0$.

Equation (8a) simply states that the electrons which arrive at location k at time n are the sum of three contributions: electrons which were at a previous location $k-k_e$ at time $n-1$; their electron offsprings, each of which is independently generated with probability $P[k]$: and hole-generated electrons each of which is independently generated with probability $Q[k]$. Similarly (8b) states that the holes which arrive at location k at time n are the sum of the holes which were at the location $k+k_h$ at time $n-1$ and their hole offsprings as well as the holes which are generated by the electrons at location $k-k_e$ at time $n-1$.

It is convenient to regard the set of functions, $\{Z[k,n]\}$, $\{Y[k,n]\}$, $\{z[k,n]\}$, and $\{y[k,n]\}$, for $k = 1,\cdots,L$, as components of vector random processes all varying only in time

$$\boldsymbol{X}^T[n] \equiv (\boldsymbol{Z}^T[n], \boldsymbol{Y}^T[n]) \quad \text{and} \quad \boldsymbol{x}^T[n] \equiv (\boldsymbol{z}^T[n], \boldsymbol{y}^T[n]) \quad (9)$$

where $\boldsymbol{Z}^T[n] \equiv (Z[1,n], Z[2,n], \cdots, Z[L,n])$, $\boldsymbol{Y}^T[n] \equiv (Y[1,n], Y[2,n], \cdots, Y[L,n])$, $\boldsymbol{z}^T[n] \equiv (z[1,n], z[2,n], \cdots, z[L,n])$, $\boldsymbol{y}^T[n] \equiv (y[1,n], y[2,n], \cdots, y[L,n])$. Equations (8a) and (8b) can then be put in the form

$$\boldsymbol{Z}[n] = \mathsf{S}_-\{\boldsymbol{Z}[n-1]\} + \mathsf{S}_-\{\boldsymbol{z}[n-1]\} + \mathsf{S}_+\{\boldsymbol{y}[n-1]\} \quad (10a)$$

$$\boldsymbol{Y}[n] = \mathsf{S}_+\{\boldsymbol{Y}[n-1]\} + \mathsf{S}_+\{\boldsymbol{y}[n-1]\} + \mathsf{S}_-\{\boldsymbol{z}[n-1]\} \quad (10b)$$

where S_- and S_+ are the operators that shift the elements of a vector by k_e and $-k_h$, respectively, and fills the empty location with zeros, as can be easily seen in (8a) and (8b). Equivalently,

$$\boldsymbol{X}[n] = \boldsymbol{A}\boldsymbol{X}[n-1] + \boldsymbol{B}\boldsymbol{x}[n-1] \quad (10c)$$

where $\boldsymbol{A}$ and $\boldsymbol{B}$ are properly selected matrices.

Conditioned on $\boldsymbol{X}[n]$ the elements of $\boldsymbol{x}[n-1]$ are independent Binomial random variables. For single electron injection, $\boldsymbol{X}^T[0] = (1,0,\cdots,0;0,\cdots,0)$. As (10c) indicates, the statistics of $\boldsymbol{X}[n]$ can be solely determined from the statistics of $\boldsymbol{X}[n-1]$, so that $\boldsymbol{X}[n]$ is a Markov vector process [40], [41]. The moments of $\boldsymbol{X}[n]$, $\boldsymbol{m}_x[n] \equiv E\{\boldsymbol{X}[n]\}$ and $\boldsymbol{R}_{xx}[n,m] \equiv E\{\boldsymbol{X}[n]\boldsymbol{X}^T[m]\}$, are directly related to the moments $m_Z[k,n]$, $m_Y[k,n]$, $R_{ZZ}[k,j;n,m]$, $R_{YY}[k,j;n,m]$, and $R_{ZY}[k,j;n,m]$.

III. Statistics of The Impulse Response Function

A. Mean

To obtain the mean value of $\boldsymbol{X}[n]$ we take the expectation of both sides of (8a) and (8b). Conditioning the right-hand sides on $\boldsymbol{X}[n-1]$, and using the fact that given $\boldsymbol{X}[n-1]$, the elements of $\boldsymbol{x}[n-1]$ are independent binomial random variables, we obtain a recursive relation for $\boldsymbol{m}_x[n]$:

$$m_Z[k,n] = (1+P[k])m_Z[k-k_e,n-1] + Q[k]m_Y[k+k_h,n-1] \quad (11a)$$

$$m_Y[k,n] = (1+Q[k])m_Y[k+k_h,n-1] + P[k]m_Z[k-k_e,n-1] \quad (11b)$$

for $k = 1,\cdots,L$ and $n = 0,\cdots,\infty$. The initial condition is $\boldsymbol{m}_X^T[n] = (1,0,\cdots,0;0,\cdots,0)$. The boundary conditions require that $m_Z[k,n]$ and $m_Y[k,n]$ are zero for $k \notin [1,L]$. Equations (11a,b) can be easily computed and $m_h[n]$ can be found from (3).

1) Transport Equations: In the limit when the number of spatial cells are very large ($L \to \infty$ and $\Delta x \to 0$) and the ionization probabilities are very small, so that

$$\frac{P[k]}{k_e\Delta x} \to \alpha(x), \quad \frac{Q[k]}{k_h\Delta x} \to \beta(x), \quad (12a)$$

$$L\Delta x \to W, \quad k\Delta x \to x, \quad \text{and} \quad n\Delta t \to t, \quad (12b)$$

the mean number of electrons and holes approach to the mean electron/hole densities, $m_Z(x,t)$ and $m_Y(x,t)$, respectively,

$$\frac{m_Z[k,n]}{\Delta x} \to m_Z(x,t) \quad \text{and} \quad \frac{m_Y[k,n]}{\Delta x} \to m_Y(x,t). \quad (13)$$

From (11), we obtain the well-known carrier transport equations

$$\frac{\partial J_e(x,t)}{\partial x} + \frac{1}{v_e}\frac{\partial J_e(x,t)}{\partial t} = \alpha(x)J_e(x,t) + \beta(x)J_h(x,t) \quad (14a)$$

$$\frac{\partial J_h(x,t)}{\partial x} - \frac{1}{v_h}\frac{\partial J_h(x,t)}{\partial t} = \alpha(x)J_e(x,t) + \beta(x)J_h(x,t) \quad (14b)$$

where $J_e(x,t) = qv_e m_Z(x,t)$ and $J_h(x,t) = qv_h m_Y(x,t)$. Once $J_e(x,t)$ and $J_h(x,t)$ are determined, the total current induced in the external circuit that results from charge transport within the device is

$$J(t) = \frac{1}{W}\int_{x=0}^{W} [J_e(x,t) + J_h(x,t)]\,dx. \tag{15}$$

These equations were independently derived earlier [33] and were solved for arbitrary APD architectures with position-dependent ionization rates and distributed carrier injection [27], [28].

B. Variance

Using (8a) and (8b), an equation for the function $\boldsymbol{R}_{xx}[n,n] = E\{\boldsymbol{X}[n]\boldsymbol{X}^T[n]\}$ can be derived in terms of $\boldsymbol{R}_{xx}[n-1,n-1]$ by taking conditional expectations as was done for the mean. The result can be cast in terms of $R_{ZZ}[k,j;n,n]$, $R_{YY}[k,j;n,n]$, and $R_{ZY}[k,j;n,n]$:

$$\begin{aligned}
R_{ZZ}[k,j;n,n] = {} & (1+P[k])(1+P[j]) \\
& \cdot R_{ZZ}[k-k_e, j-k_e; n-1, n-1] \\
& + \delta_{k,j}\{P[k](1-P[k])m_Z[k-k_e, n-1]\} \\
& + Q[k]Q[j] \\
& \cdot R_{YY}[k+k_h, j+k_h; n-1, n-1] \\
& + \delta_{k,j}\{Q[k](1-Q[k])m_Y[k+k_h, n-1]\} \\
& + (1+P[k])Q[j] \\
& \cdot R_{ZY}[k-k_e, j+k_h; n-1, n-1] \\
& + (1+P[j])Q[k] \\
& \cdot R_{ZY}[j-k_e, k+k_h; n-1, n-1]
\end{aligned} \tag{16a}$$

$$\begin{aligned}
R_{YY}[k,j;n,n] = {} & P[k]P[j] \\
& \cdot R_{ZZ}[k-k_e, j-k_e; n-1, n-1] \\
& + \delta_{k,j}\{P[k](1-P[k])m_Z[k-k_e, n-1]\} \\
& + (1+Q[k])(1+Q[j]) \\
& \cdot R_{YY}[k+k_h, j+k_h; n-1, n-1] \\
& + \delta_{k,j}\{Q[k](1-Q[k])m_Y[k+k_h, n-1]\} \\
& + P[k](1+Q[j]) \\
& \cdot R_{ZY}[k-k_e, j+k_h; n-1, n-1] \\
& + P[j](1+Q[k]) \\
& \cdot R_{ZY}[j-k_e, k+k_h; n-1, n-1]
\end{aligned} \tag{16b}$$

$$\begin{aligned}
R_{ZY}[k,j;n,n] = {} & (1+P[k])P[j] \\
& \cdot R_{ZZ}[k-k_e, j-k_e; n-1, n-1] \\
& + \delta_{k,j}\{P[k](1-P[k])m_Z[k-k_e, n-1]\} \\
& + (1+Q[j])Q[k] \\
& \cdot R_{YY}[k+k_h, j+k_h; n-1, n-1] \\
& + \delta_{k,j}\{Q[k](1-Q[k])m_Y[k+k_h, n-1]\} \\
& + (1+P[k])(1+Q[j]) \\
& \cdot R_{ZY}[k-k_e, j+k_h; n-1, n-1] \\
& + P[j]Q[k] \\
& \cdot R_{ZY}[j-k_e, k+k_h; n-1, n-1]
\end{aligned} \tag{16c}$$

for all $k,j = 1,\ldots,L$.

Here δ denotes Kronecker-delta. The initial conditions are $R_{ZZ}[k,j;0,0] = \delta_{k,1}\delta_{j,1}$, $R_{YY}[k,j;0,0] = R_{ZY}[k,j;0,0] = 0$, for all $k,j \in [1,L]$. Boundary conditions are $R_{ZZ}[k,j;n,n] = R_{YY}[k,j;n,n] = R_{ZY}[k,j;n,n] = 0$, for $k,j \notin [1,L]$. Using (4) with $m = n$, the $R_{hh}[n,n]$ can be evaluated, and current variance can be found from (5). These equations can be computed recursively. $P[k]$ and $Q[k]$ can be used to approximate $\alpha(x)$ and $\beta(x)$ for conventional APD's where ionizations occur continuously, or can be directly used for multilayer APD's where ionizations take place only at the energy band-gap discontinuities.

Differential Equations: In the limit described in (12), neglecting the terms with second-order coefficients, we define the autocorrelation and crosscorrelation of the electron and hole densities at two different locations at the same time as

$$\begin{aligned}
&\frac{R_{ZZ}[k,j;n,n]}{\Delta x^2} \to R_{ZZ}(x_1,x_2;t), \\
&\frac{R_{YY}[k,j;n,n]}{\Delta x^2} \to R_{YY}(x_1,x_2;t), \quad \text{and} \\
&\frac{R_{ZY}[k,j;n,n]}{\Delta x^2} \to R_{ZY}(x_1,x_2;t).
\end{aligned}$$

Then, we transform the difference equations (16) into partial differential equations

$$\begin{aligned}
v_e\left[\frac{\partial R_{ZZ}}{\partial x_1} + \frac{\partial R_{ZZ}}{\partial x_2}\right] + \frac{\partial R_{ZZ}}{\partial t} = {} & \\
v_e[\alpha(x_1) + \alpha(x_2)]R_{ZZ}(x_1,x_2,t) & \\
+ v_h\{\beta(x_2)R_{ZY}(x_1,x_2,t) & \\
+ \beta(x_1)R_{ZY}(x_2,x_1,t)\} & \\
+ v_e\alpha(v_e t)\delta(x_1 - v_e t)\delta(x_2 - v_e t) &
\end{aligned} \tag{17a}$$

$$\begin{aligned}
-v_h\left[\frac{\partial R_{YY}}{\partial x_1} + \frac{\partial R_{YY}}{\partial x_1}\right] + \frac{\partial R_{YY}}{\partial t} = {} & \\
v_h[\beta(x_1) + \beta(x_2)]R_{ZZ}(x_1,x_2,t) & \\
+ v_e\{\alpha(x_2)R_{ZY}(x_1,x_2,t) & \\
+ \alpha(x_1)R_{ZY}(x_2,x_1,t)\} & \\
+ v_e\alpha(v_e t)\delta(x_1 - v_e t)\delta(x_2 - v_e t) &
\end{aligned} \tag{17b}$$

$$\begin{aligned}
v_e\frac{\partial R_{ZY}}{\partial x_1} - v_h\frac{\partial R_{ZY}}{\partial x_2} + \frac{\partial R_{ZY}}{\partial t} = {} & \\
[1 + v_e\alpha(x_1) + v_h\beta(x_2)]R_{ZY}(x_1,x_2,t) & \\
+ v_e\alpha(x_2)R_{ZZ}(x_1,x_2,t) & \\
+ v_h\beta(x_1)R_{YY}(x_1,x_2,t)\} & \\
+ v_e\alpha(v_e t)\delta(x_1 - v_e t)\delta(x_2 - v_e t) &
\end{aligned} \tag{17c}$$

where $\alpha(x) = 0$, and $\beta(x) = 0$ for $x_1, x_2 \notin [0,W]$, and $t > 0$. The initial conditions are $R_{ZZ}(x_1,x_2,0) = \delta(x_1)\delta(x_2)$, and $R_{YY}(x_1,x_2,0) = R_{ZY}(x_1,x_2,0) = 0$. The boundaries are removed by letting $\alpha(x) = 0$, and $\beta(x) = 0$ for $x_1, x_2 \notin [0,W]$. These differential equations (in the sense of distributions) have not yet been solved analytically. However, the original equations in (16) are a set of first-order finite-difference equations [42].

C. Autocorrelation

Determination of the autocorrelation function of the impulse-response $\mathbf{R}_{hh}[n,m]$ requires knowledge of $\boldsymbol{R}_{xx}[n,m]$. Again $\boldsymbol{R}_{xx}[n,m]$ can be obtained from $\boldsymbol{R}_{xx}[n,m-1]$ for all n, and $m=n+1, n+2, \cdots, L$. For $m>n$, by using (8), and taking properly ordered conditional expectations, one can show that:

$$R_{ZZ}[k,j;n,m] = (1+P[j])R_{ZZ}[k,j-k_e;n,m-1] + Q[j]R_{ZY}[k,j+k_h;n,m-1]. \quad (18a)$$

$$R_{YY}[k,j;n,m] = (1+Q[j])R_{YY}[k,j+k_e;n,m-1] + P[j]R_{ZY}[j-k_e,k;m-1,n]. \quad (18b)$$

$$R_{ZY}[k,j;n,m] = (1+Q[j])R_{ZY}[k,j+k_e;n,m-1] + P[j]R_{ZZ}[k,j-k_e;n,m-1]. \quad (18c)$$

$$R_{ZZ}[k,j;n,m] = (1+P[j])R_{ZY}[k-k_e,j;m-1,n] + Q[k]R_{YY}[k+k_h j;m-1,n]. \quad (18d)$$

for all $k,j=1,\cdots,L$.

Also $R_{ZZ}[k,j;n,m]$ and $R_{YY}[k,j;n,m]$ are symmetric, i.e., $R_{ZZ}[k,j;n,m]=R_{ZZ}[k,j;m,n]$ and $R_{YY}[k,j;n,m]=R_{YY}[k,j;m,n]$. The initial points for these recursion relations are given by $\boldsymbol{R}_{xx}[n,n]$ which are already found for all n using (16). Boundary conditions are $R_{ZZ}[k,j;n,m]=R_{YY}[k,j;n,m]=R_{ZY}[k,j;n,m]=0$, for $k,j\notin[1,L]$. The autocorrelation function of the impulse response $R_{hh}[n,m]$ can be easily computed using (4).

Differential Equations: In the limit described by (12), we write partial differential equations for the autocorrelation and cross-correlation functions of the electron and hole densities at two different locations and times, i.e., for $R_{ZZ}(x_1,x_2;t_1,t_2)$, $R_{YY}(x_1,x_2;t_1,t_2)$, and $R_{ZY}(x_1,x_2;t_1,t_2)$:

$$\left(v_e\frac{\partial}{\partial x_2}+\frac{\partial}{\partial t_2}\right)R_{ZZ}(x_1,x_2;t_1,t_2) = v_e\alpha(x_2)\cdot R_{ZZ}(x_1,x_2;t_1,t_2)+v_h\beta(x_2)R_{ZY}(x_1,x_2;t_1,t_2) \quad (19a)$$

$$\left(-v_h\frac{\partial}{\partial x_2}+\frac{\partial}{\partial t_2}\right)R_{YY}(x_1,x_2;t_1,t_2) = v_h\beta(x_2)\cdot R_{YY}(x_1,x_2;t_1,t_2)+v_e\alpha(x_2)R_{ZY}(x_2,x_1;t_1,t_2) \quad (19b)$$

$$\left(-v_h\frac{\partial}{\partial x_2}+\frac{\partial}{\partial t_2}\right)R_{ZY}(x_1,x_2;t_1,t_2) = v_h\beta(x_2)\cdot R_{ZY}(x_1,x_2;t_1,t_2)+v_e\alpha(x_2)R_{ZZ}(x_1,x_2;t_1,t_2) \quad (19c)$$

$$\left(v_e\frac{\partial}{\partial x_1}+\frac{\partial}{\partial t_1}\right)R_{ZY}(x_1,x_2;t_1,t_2) = v_e\alpha(x_1)\cdot R_{ZY}(x_1,x_2;t_1,t_2)+v_h\beta(x_1)R_{ZZ}(x_1,x_2;t_1,t_2). \quad (19a)$$

Values at $t_1=t_2=t>0$ for $x_1,x_2\in[0,W]$ can be obtained by solving (17).

D. Probability Generating Function of X[n]

The probability generating function of $\boldsymbol{X}[n]$ is

$$G_n(\boldsymbol{s},\boldsymbol{w}) = E\left\{\prod_{k=1}^{L} s_k^{Z[k,n]}w_k^{Y[k,n]}\right\} \quad (20)$$

where $\boldsymbol{s}=(s_1,s_2,\cdots,s_L)$ and $\boldsymbol{w}=(w_1,w_2,\cdots,w_L)$. To relate G_n to G_{n-1}, we take the expectation in (20) by conditioning on $\boldsymbol{X}[n-1]$

$$G_n(\boldsymbol{s},\boldsymbol{w}) = E\left\{E\left\{\prod_{k=l}^{L} s_k^{Z[k,n]}w_k^{Y[k,n]}]|\boldsymbol{X}[n-1]\right\}\right\}$$

and by using (8) and grouping the s_k and w_k terms of the same power, we obtain

$$= E\left\{E\left\{\prod_{k=1}^{L}(s_kw_k)^{(Z[k-k_e,n-1]+y[k+k_h,n-1])}\cdot s_k^{Z[k-k_e,n-1]}w_k^{Y[k+k_h,n-1]}|\boldsymbol{X}[n-1]\right\}\right\}.$$

Since, conditioned on $\boldsymbol{X}[n-1]$, $z[k-k_e,n-1]$ and $y[k+k_h,n-1]$ are independent binomial random variables with populations $Z[k-k_e,n-1]$ and $Y[k+k_h,n-1]$ and probabilities $P[k]$ and $Q[k]$, respectively, so that

$$= E\left\{\prod_{k=1}^{L} s_k^{Z[k-k_e,n-1]}w_k^{Y[k+k_h,n-1]}\cdot G_z(s_kw_k)^{Z[k-k_e,n-1]}G_y(s_kw_k)^{Y[k+k_h,n-1]}\right\}$$

where $G_z(s)=(1-P[k]+sP[k])$ and $G_y(s)=(1-Q[k]+sQ[k])$ denote the probability generating function of z and y, respectively. Substituting for $G_z(s=s_kw_k)$ and $G_y(s=s_kw_k)$,

$$= E\left\{\prod_{k=1}^{L}\{s_k(1-P[k]+s_kw_kP[k])\}^{Z[k-k_e,n-1]}\cdot\{w_k(1-Q[k]+s_kw_kQ[k])\}^{Y[k+k_h,n-1]}\right\}$$

from which we obtain

$$G_n(s_1,\cdots,s_L,w_1,\cdots,w_L) = G_{n-1}(f_1,f_2,\cdots,f_Lg_1,g_2,\cdots,g_L), \quad (21)$$

where

$$f_j=\begin{cases} s_{j+k_e}(1-P[j+k_e] \\ \quad +s_{j+k_e}w_{j+k_e}P[j+k_e]) & \text{if } j<L-k_e \\ 1 & \text{if } j\geq L-k_e \end{cases}$$

and

$$g_j=\begin{cases} w_{j-k_h}(1-Q[j-k_h] \\ \quad +s_{j-k_h}w_{j-k_h}Q[j-k_h]) & \text{if } j>k_h \\ 1 & \text{if } j\leq k_h \end{cases}$$

with $G_0(\boldsymbol{s},\boldsymbol{t})=s_1$, for single-electron injection.

In principle one can obtain $\boldsymbol{m}_x[n]$ by taking the first partial derivative of $G_n(\boldsymbol{s}, \boldsymbol{w})$ with respect to s_k and w_k. Using the recursion formula in (21) and chain differentiation one can derive the same recursion equations for the mean number of carriers as in (11). Also one can take double partial derivatives of $G_n(\boldsymbol{s}, \boldsymbol{w})$ with respect to all pairs of s_k and w_k, and derive the same recursive equations for $\boldsymbol{R}_{xx}[n, n]$ as in (16). Higher order moments can be similarly obtained.

IV. Examples

The foregoing equations are applicable to APD's with arbitrary structures. Although the boundary conditions were set for a single-electron injection at $x = 0$, these equations are still valid for double-carrier or distributed injection, and dark noise. We illustrate our theory with two APD structures: a conventional APD (CAPD) and a multiquantum well APD (MQW-APD) with the same mean gain ($M = 5$) and carrier ionization rate ratio ($\frac{\alpha}{\beta} = \frac{P}{Q} = 4.5$).

A. Conventional APD

For simplicity, we only consider a single-layer CAPD with single electron injection at the multiplication region edge ($x = 0$) and assume constant carrier ionization rates $\alpha = 6300\ \mathrm{cm}^{-1}$ and $\beta = 1400\ \mathrm{cm}^{-1}$, and uniform carrier velocities $v_e = 10^7\mathrm{cm}/$ and $v_h = 5 \times 10^6\mathrm{cm/s}$. The multiplication region width is $W = 2\,\mu\mathrm{m}$.

1) Mean Impulse Response: We have computed the mean current $m_h(t)$ by using (11) and (3) with $L = 100$, $k_e = 2$, and $k_h = 1$. The ionization rates α and β correspond to $P = \exp[\alpha k_e \Delta x] - 1 = 0.02552$ and $Q = \exp[\beta k_h \Delta x] - 1 = 0.002804$, respectively. The time increment used in this computation was $\Delta t = \frac{\Delta x}{v_h} = 0.4\,\mathrm{ps}$.

The mean current response is in Fig. 3(a). It rises sharply to the solid curve peak at the electron transit time, $t = \tau_e = 20$ ps, drops abruptly, and decays slowly with a long tail extending beyond τ_e to about 100 ps as a result of the avalanche buildup time. The corner points following the peak correspond to secondary arrivals of electrons and holes.

The Fourier transform of the mean current response is shown in Fig. 3(b). It has a full-width-half-maximum (FWHM) bandwidth of 10 GHz.

To verify our computations we computed the mean gain (the area under the mean current divided by q) and compared it to its theoretical value [1]–[4]

$$M_e = \frac{\alpha - \beta}{-\beta + \alpha e^{-(\alpha-\beta)W}} = 5.08. \tag{22}$$

Our computations gave 5.10.

2) *Variance and Signal-to-Noise Ratio (SNR) of the Impulse Response:* We have computed the variance of the impulse response $\sigma_h^2(t)$ by using (16a, b, c), (4), and (5). The standard deviation of the current $\sigma_h(t)$ is the dashed curve in Fig. 3(a). It is lowest at the onset of the response, where multiplication noise has not yet accumulated. It peaks at the same time as the mean current, and subsequently decreases at a much slower rate and with greater value. This gradual decay of $\sigma_h(t)$ may be attributed to the uncertainties accumulated during the first

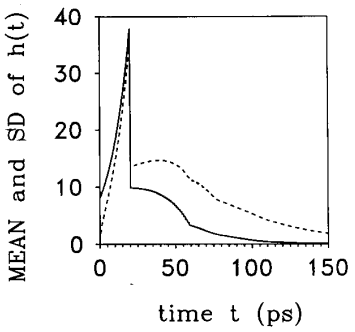

(a)

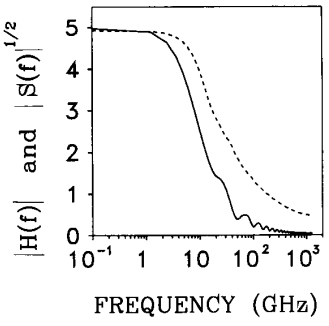

(b)

Fig. 3. (a) Time dependence of the mean (solid line) and the standard deviation (dashed line) of the impulse response of a CAPD. (b) The Fourier transform of the mean response to a single photon (solid line, in units of q) and the power spectral density (dashed line, in units of q) of the photoelectric current corresponding to an optical power normalized to give $\mu = 1$. The unscaled magnitude of the power spectral density corresponding to any μ can be found by multiplying by $q\mu^{1/2}$.

τ_e seconds that do not die off as rapidly as the mean current itself. For a high-data digital-optical communication-system, this type of noise will enhance intersymbol interference and limit the bit-error-rates.

Another measure of performance is the signal-to-noise ratio of the current, $\mathrm{SNR}(t) = \frac{m_h^2(t)}{\sigma_h^2(t)}$, shown in Fig. 4(a). This function is large for a short time duration and decreases rapidly to zero with a step jump at $t = \tau_e$.

Knowledge of the mean and the variance of the impulse response is generally not sufficient to evaluate the bit-error-rate in a digital optical communication system using these detectors. Because the response to a random sequence of photons representing a pulse of light is the sum of the electric pulses generated by each of the photons, the properties of the photoelectric current at any time is determined not only by the mean and the variance of $h(t)$, but requires knowledge of its autocorrelation function as well.

3) Autocorrelation and Correlation Coefficient of the Impulse Response: The autocorrelation of the impulse $R_{hh}(t_1, t_2)$ has been computed by using (4) and (18). As shown in Fig. 5, at pairs of times $t_1, t_2 < \tau_e$ the autocorrelation is large but diminishes as t_1 or t_2 increases. An indication of the degree of coherence of the impulse response at different pairs of times

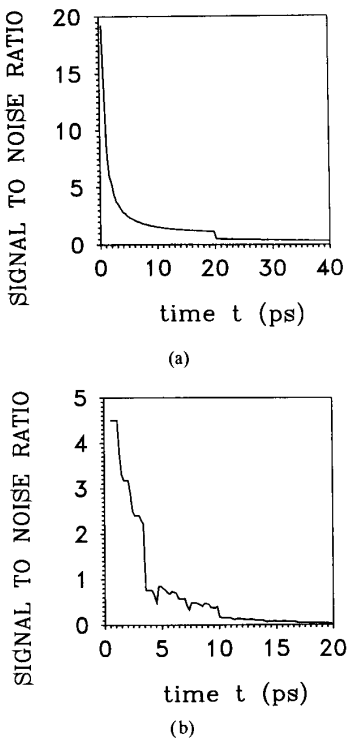

Fig. 4. Time dependence of the signal-to-noise ratio of the current response of (a) a CAPD, (b) an MQW-APD.

is obtained by computing the correlation coefficient

$$r(t_1,t_2)=\frac{C(t_1,t_2)}{\sqrt{C(t_1,t_1)C(t_2,t_2)}},$$

$$\text{where } C(t_1,t_2)=R_{hh}(t_1,t_2)-m_h(t_1)m_h(t_2).$$

As in Fig. 6, the current is weakly correlated for $0<t_1<\tau_e$ and $0<t_2<\tau_e$, and thereafter becomes more correlated. The reason is that at the onset of the multiplication process the ionization events are relatively independent, whereas later ionizations become more correlated since they share a common origin.

To verify our results we computed the volume under the current autocorrelation function $R_{hh}(t_1,t_2)$ to obtain the second moment of the gain. We then calculated the excess noise factor for single-electron carrier injection, and compared it to its theoretical value [5]

$$F_e=\frac{M_2}{M^2}=k_cM+\left(2-\frac{1}{M}\right)(1-k_c)=2.53. \quad (23)$$

Our computation gave 2.5.

B. Multiquantum-Well APD

A simple MQW-APD with four GaInAs/AlInAs stages is shown in Fig. 7. Each layer thickness is 500 A° and the total width is 3500 A°. The electron and hole ionization probabilities at each ionization stage are $P=0.3340$ and $Q=0.07422$, respectively. Electron and hole velocities are 10^7 cm/s and 5×10^6 cm/s, respectively. Single electron injection is assumed at the multiplication region boundary ($x=0$).

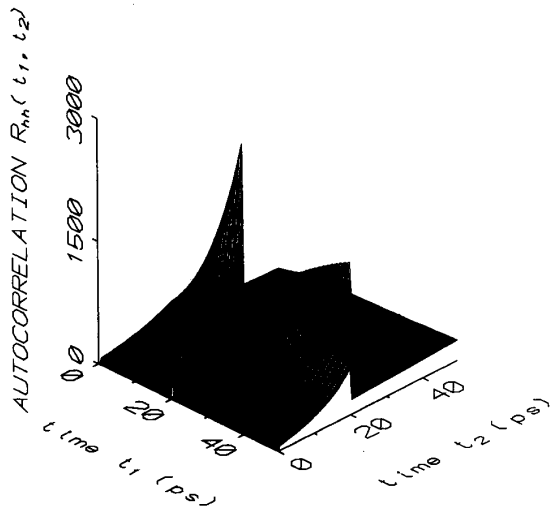

Fig. 5. The autocorrelation function $R_{hh}(t_1,t_2)$ of the impulse response for CAPD.

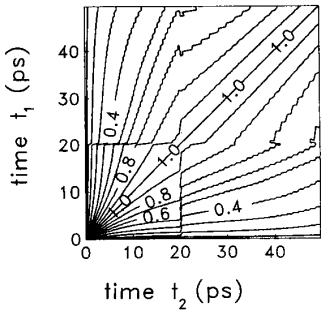

Fig. 6. Contours of constant correlation coefficient $r_{hh}(t_1,t_2)$ of CAPD current response.

1) Mean Impulse Response: We have computed the mean current $m_h(t)$ by using (3) and (11) with $L=35$, $k_e=2$, and $k_h=1$. The time increment Δt used in this computation was 0.2 ps. Electrons can only ionize at four locations, $k=5$, 15, 25, 35, and holes can ionize at $k=1$, 11, 21, 31. Accordingly,

$$P(k)=\begin{cases}P & \text{if } k=5,15,25,35\\ 0 & \text{otherwise}\end{cases}$$

and

$$Q(k)=\begin{cases}Q & \text{if } k=1,11,21,31\\ 0 & \text{otherwise.}\end{cases}$$

These locations correspond to the energy band-gap transitions in the multilayer GaInAs/AlInAs crystals. Electrons ionize upon entering the AlInAs layers and holes ionize upon entering GaInAs layers.

The mean current response is the solid curve in Fig. 8(a). As in the conventional case, it rises sharply to a peak, drops abruptly at $t=\tau_e=3.5$ ps, and decays slowly thereafter. The discontinuities at $t>\tau_e$ are due to secondary arrivals

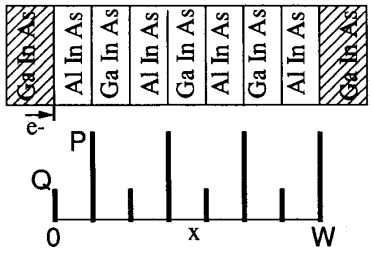

Fig. 7. A MQW-APD with four GaInAs/AlInAs stages. Each layer thickness is 500 A° and the total width is 3500 A°. $P = 0.3340$ and $Q = 0.07422$.

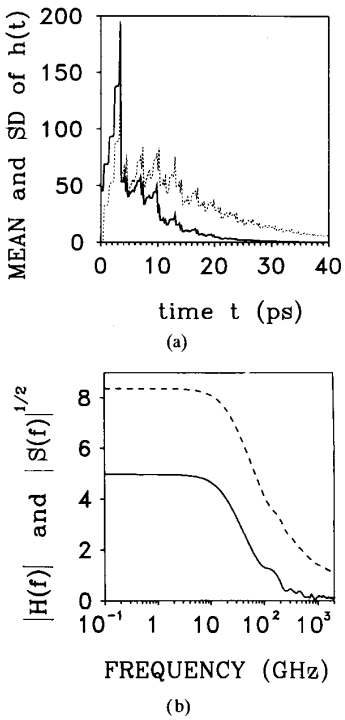

Fig. 8. (a) Time dependence of the mean (solid line) and the standard deviation (dashed line) of the impulse response of a MQW-APD. (b) The Fourier transform of the mean response to a single photon (solid line, in units of q) and the power spectral density (dashed line, in units of q) of the photoelectric current corresponding to an optical power normalized to give $\mu = 1$. The magnitude of the power spectral density corresponding to any μ can be found by multiplying it by $q\mu^{1/2}$.

of electrons and holes. The mean response diminishes much faster and attains greater magnitudes than that in conventional device with the same gain. The Fourier transform of the current response is plotted in Fig. 8(b). The FWHM bandwidth of frequency response is 40 GHz.

To verify our results we have computed the mean gain M (the area under the mean current function) and compared it to its theoretical value [5]

$$M = \frac{(P-Q)(1+P)^N}{P(1+Q)^{N+1} - Q(1+P)^{N+1}} = 5.00 \qquad (24)$$

where N is the number of ionization stages. Our computation was 5.00.

2) Variance and Signal-to-Noise Ratio of the Impulse Response: We have computed the variance of the impulse response $\sigma_h^2(t)$ by using (4), (5), and (16). The standard deviation of the current $\sigma_h(t)$ is the dashed curve in Fig. 8(a). It is zero until the injected electron ionizes for the first time. As for the CAPD, $\sigma_h(t)$ does not decay as rapidly as the mean current. It diminishes faster than that of the CAPD but it reaches larger magnitudes.

To compare the two devices we examine their signal-to-noise ratios depicted in Fig. 4. The CAPD has a higher SNR at any time, even though it has a greater excess noise factor F. This may at first appear to be inconsistent. The SNR at time t is a measure of the instantaneous uncertainty, whereas F is a global measure integrated over the device response time. The fact that the CAPD has higher SNR (i.e., lower instantaneous noise) but higher F (i.e., greater averaged noise) is a result of its noise being more correlated over its response time than in the MQW-APD. Thus, if the CAPD and MQW-APD were to have the same response time, the former would be more suitable for faster applications than the latter! Clearly, this is not so, since MQW-APD's are designed to have shorter response time. The instantaneous noise (or SNR) of the CAPD is less because the probability of ionization within a time increment is very low in comparison with localized high-probability ionizations in the MQW-APD.

For improved performance, the SNR of a pulse should be large within the period of time in which most of its energy is contained. In the conventional case, most of the signal energy is within 60 ps and the SNR is greater than one for $t <$ 20 ps; whereas in the superlattice case, most of the energy is within 10 ps and the SNR is greater than one for $t < 3.5$ ps. Thus, the CAPD has greater SNR within the time scale it is utilized. The MQW-APD may be preferred for its speed and lower excess noise factor in detection circuits with long integration times, but not for its SNR when the detection is instantaneous.

3) Autocorrelation and the Correlation Coefficient of the Impulse Response: The impulse response autocorrelation $R_{hh}(t_1, t_2)$ has been computed by using (4) and (18). As shown in Fig. 9, for $0 < t_1 < \tau_e$ and $0 < t_2 < \tau_e$ the autocorrelation is large but it diminishes as t_1 or t_2 increases. The correlation coefficient plot in Fig. 10 clearly show that the MQW-APD response has weaker correlation than that of CAPD.

To verify our results we computed the volume under the current autocorrelation function to obtain the second moment of the gain. We then calculated the excess noise factor for single-electron carrier injection, and compared it to its theoretical value [5]

$$F_e = \frac{M_2}{M^2} = 1 + \frac{\left(1-\frac{1}{M}\right)\left(1-\frac{Q}{P}\right)}{2+P+Q} \cdot \left\{-P + 2\frac{1-PQ}{1+Q}\left[M\frac{Q(1+P)}{P-Q} + \frac{1}{1+P}\right]\right\} = 2.161. \qquad (25)$$

Our computation gave 2.161.

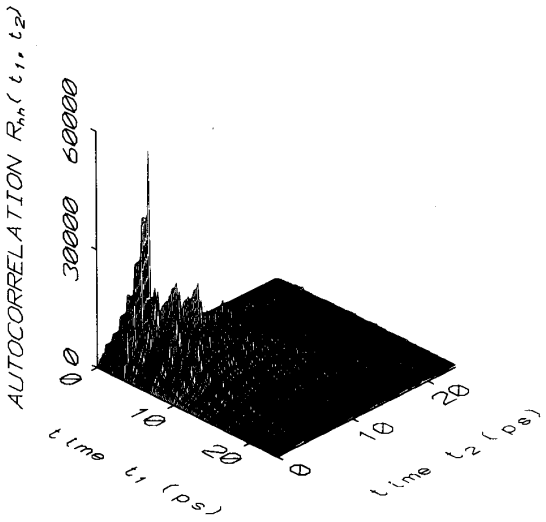

Fig. 9. The autocorrelation function $R_{hh}(t_1, t_2)$ of the impulse response for a MQW-APD.

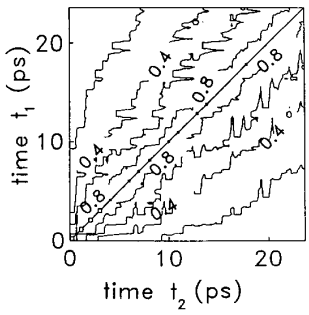

Fig. 10. Contours of constant correlation coefficient $r_{hh}(t_1, t_2)$ of MWQ-APD current response.

V. Photoelectric Current

The previous analysis dealt with the response $h(t)$ of the device to a single absorbed photon. Under a steady light illumination of power P, the total photoelectric current $i(t)$ is a sequence of electric pulses $h(t)$ beginning at the times of injection of the photogenerated electrons. If the incident photon stream is described by a Poisson point process with rate ϕ and the quantum efficiency is η, then the photoelectron injection is another Poisson point process with intensity $\mu = \eta\phi$, and $i(t)$ is a filtered Poisson process (shot noise) [40]. The total photocurrent $i(t)$ is then

$$i(t) = \sum_n h_n(t - t_n) \tag{26}$$

where $\{t_n\}$ are the electron injection times and $\{h_n(t - t_n); t \geq t_n\}$, for $n = 1, 2, \cdots$ are statistically independent, identically distributed random processes all having the same distributions as the process $h(t)$ described in earlier sections. The mean, the variance, and the covariance function of $i(t)$ can be shown to be

$$m_i = \mu \int_0^\infty m_h(t)\, dt = q\mu M \tag{27}$$

$$\sigma_i^2 = \mu \int_0^\infty E\{h^2(t)\}\, dt \tag{28}$$

$$C_i(\tau) \equiv C_{ii}(t, t+\tau) = \mu \int_0^\infty R_{hh}(t', t'+\tau)\, dt' \tag{29}$$

respectively. The moments of $i(t)$ are thus readily obtained once the moments of $h(t)$ are found. The power spectral density $S_i(f)$ of the photoelectric current is the Fourier transform of $C_i(\tau)$ and the circuit bandwidth is

$$B \equiv \frac{\int_0^\infty E\{h^2(t)\}\, dt}{2\left\{\int_0^\infty m_h(t)\, dt\right\}^2} = \frac{\mu\sigma_i^2}{2m_i^2}. \tag{30}$$

Numerical Results: We have computed the mean, the variance, and the covariance of the photoelectric current corresponding to an optical power $P = 1$ mW at wavelength $\lambda = 1.3$ μm, and assuming unity quantum efficiency ($\eta = 1$). For the CAPD, the mean and the standard deviation of the photocurrent are 5.23 mA and 14 μA, respectively, and the circuit bandwidth B is 23 GHz. For the MQW-APD, the mean and the standard deviation of the photocurrent are 5.23 mA and 28 μA, respectively, and circuit bandwidth B is 93 GHz. The power spectral density of $i(t)$ for both devices are the dashed curves in Figs. 3(b) and 8(b), respectively. The FWHM bandwidths are 27 GHz for CAPD and 100 GHz for MQW-APD which are in close agreement with the calculated values. The photocurrent generated in the CAPD has a narrower power spectral density but a higher signal-to noise ratio.

VI. Conclusion

We have determined a discrete stochastic model to describe the dynamics of the double-carrier multiplication process in APD's with arbitrary structure (conventional and superlattice). Based on this model, we derived recursive equations to compute the mean, the variance, and the autocorrelation function of the impulse response, assuming single-electron injection. In the limit of very large grid size, we have transformed the difference equations into differential equations describing the mean, the variance, and the autocorrelation function of the impulse response. Analytical solutions for these differential equations are found only for the mean current.

We applied our analysis to a conventional APD (CAPD) and a simple multiquantum-well APD (MQW-APD) with the same mean gain and carrier ionization ratio. For both devices we computed the mean, the variance, the SNR, and the autocorrelation function of the electric current pulse resulting from the injection of a single electron. A comparison between the two devices showed that the MQW-APD has a faster

response and lower excess-noise factor. However, the signal-to-noise ratio and the correlation of the current response for the CAPD was greater.

Finally, we computed the mean, the variance, the autocovariance function, and the power spectra of the photocurrent generated by coherent light of uniform power. The photocurrent generated in the CAPD has a narrower power spectral density but a higher signal-to-noise ratio.

ACKNOWLEDGMENT

The authors thank A. S. Johnson, A. Hayat, Professor P. Ney, and Professor T. Kurtz, for the useful discussions.

REFERENCES

[1] R. J. McIntyre, "Multiplication rates in uniform avalanche diodes," *IEEE Trans. Electron. Dev.*, vol. ED-13, pp. 164–168, 1966.
[2] R. J. McIntyre, "The distribution of gains in uniformly multiplying avalanche photodiodes: Theory," *IEEE Trans. Electron. Dev.*, vol. ED-19, no. 6, pp. 703–713, 1972.
[3] S. D. Personick, "New results on avalanche multiplication statistics with application to optical detection," *BELL Syst. Tech. J.* vol. 50, pp. 167–189, 1971.
[4] S. D. Personick, "Statistics of a general class of avalanche detectors with application to optical communication," *BELL Syst. Tech. J.*, vol. 50, pp. 3075–3095, 1971.
[5] M. C. Teich, K. Matsuo, and B. E. A. Saleh, "Excess noise factors for conventional and superlattice avalanche photodiodes and photomultiplier tubes," *IEEE J. Quantum Electron.*, vol. QE-22, no. 8, pp. 1184–1193, 1986.
[6] M. C. Teich, K. Matsuo, and B. E. A. Saleh, "Counting distributions and error probabilities for optical receivers incorporating superlattice avalanche photodiodes," *IEEE Trans. Electron. Dev.*, vol. ED-33, pp. 1475–1488, 1986.
[7] N. Z. Hakim, B. E. A. Saleh, and M. C. Teich, "Generalized excess noise factor for avalanche photodiodes of arbitrary structure," *IEEE Trans. Electron. Dev.*, vol. 37, no. 3, pp. 599–610, 1990.
[8] J. N. Hollenhorst, "A theory of multiplication noise," *IEEE Trans. Electron. Dev.*, vol. 37, no. 3, pp. 781–788, 1990.
[9] K. M. van Vliet, A. Friedman, and L. M. Rucker, "Theory of carrier multiplication and noise in avalanche devices-Part II: two-carrier processes," *IEEE Trans. Electron. Dev.*, vol. ED-26, pp. 752–764, 1979.
[10] K. Brennan, "Comparison of multiquantum well, graded barrier, and doped quantum well GaInAs/AlInAs avalanche photodiodes: A theoretical approach," *IEEE J. Quantum Electron.*, vol. QE-23, no. 8, pp. 1273–1282, 1987.
[11] K. Brennan, "Theory of electron and hold impact ionization in quantum well and staircase superlattice avalanche photodiode structures," *IEEE Trans. Electron. Dev.*, vol. ED-32, pp. 2197–2205, 1985.
[12] P. Chakrabarti, S. C. Choudhury, and B. B. Pal, "Noise characteristics of a superlattice avalanche photodiode," *Appl. Phys. A-Solids and Surfaces*, vol. 48, no. 4, pp. 331–334, 1989.
[13] P. Chakrabarti and B. B. Pal, "Theoretical characterization of a superlattice avalanche photodiode," *Appl. Phys. A-Solids and Surfaces*, vol. 42, no. 3, pp. 173–177, 1987.
[14] J. C. Campbell, S. Chandrasekhar, W. T. Tsang, G. J. Qua, and B. C. Johnson, "Multiplication noise of wide-bandwidth InP/InGaAsP/InGaAs avalanche photodiodes," *J. Lightwave Technol.*, vol. 7, no. 3, pp. 473–487, 1989.
[15] J. C. Campbell, A. G. Dentai, W. S. Holden, and B. L. Kasper, "High-performance avalanche photodiode with separate absorption 'grading' and multiplication regions," *Electron. Lett.*, vol. 19, pp. 818–820, 1983.
[16] F. Osaka and T. Mikawa, "Excess noise design of InP/GaInAsP/GaInAs avalanche photodiodes," *IEEE J. Quantum Electron.*, vol. QE-22, no. 3, pp. 471–478, 1986.
[17] P. P. Webb. R. J. McIntyre, and J. Conradi, "Properties of avalanche photodiodes," *RCA REV.*, vol. 35, pp. 234–278, 1974.
[18] A. M. Hayat, B. E. A. Saleh, and M. C. Teich, "Effect of dead space on gain and noise of double-carrier multiplication avalanche photodiodes," *IEEE Trans. Electron. Dev.*, pp. 546–5523, Mar. 1992.
[19] R. A. Laviolette and M. G. Staplebroek, "A non-Markovian model of a avalanche gain statistics for a solid-state photomultiplier," *J. Appl. Phys.*, vol. 65, pp. 830–836, 1989.
[20] R. A. Laviolette, "Oscillatory transients in non-Markovian random walk," *J. Chem. Phys.*, vol. 89, pp. 6905–6911, 1988.
[21] Y. Okuto and C. R. Crowell, "Threshold energy effect on avalanche breakdown voltage in semiconductor junctions," *Phys. Solid-State Electron.*, vol. 18, pp. 161–168, 1975.
[22] Y. Okuto and C. R. Crowell, "Ionization coefficients in semiconductors: A non-localized property," *Phys. Rev. B*, vol. 10, pp. 4282–4296, 1973.
[23] B. E. A. Saleh and M. C. Teich, *Fundamentals of Photonics.* New York: Wiley, 1991.
[24] B. E. Saleh, *Photoelectron Statistics.* Berlin/Heidelberg/New York: Springer-Verlag, 1978.
[25] A. M. Hayat, "Bit error rates of binary optical communication systems using avalanche photodiodes," Master's Thesis, Univ. of Wisconsin-Madison, 1988.
[26] H. L. van Trees, *Detection, Estimation and Modulation Theory, Part I.* New York: Wiley, 1968.
[27] G. Kahraman, B. E. A. Saleh, W. L. Sargeant, and M. C. Teich, "Time and frequency response of an avalanche photodiode of arbitrary structure," *IEEE Trans. Electron. Dev.*, vol. 39, pp. 553–560, Mar. 1992.
[28] M. E. Teich, W. L. Sargeant, G. Kahraman, and B. E. A. Saleh, "Optimization of a InP/InGaAsP/InGaAs separate/absorption/grading/multiplication avalanche photodiode," in preparation.
[29] M. E. Teich, K. Matsuo, and B. E. A. Saleh, "Time and frequency response of the conventional avalanche photodiode," *IEEE Trans. Electron. Dev.*, vol. ED-33, pp. 1511–1517, 1986.
[30] K. Matsuo, M. C. Teich, and B. E. A. Saleh, "Noise properties and time response of the staircase avalanche photodiode," *IEEE Trans. Electron. Dev.*, vol. ED-32, pp. 2615–2623, 1985.
[31] B. E. A. Saleh, M. M. Hayat, and M. C. Teich, "Effect of dead space on the excess noise factor and time response of avalanche photodiodes," *IEEE Trans. Electron. Dev.*, vol. 37, pp. 1976–1984, 1990.
[32] K. F. Brennan, Y. Wang, M. C. Teich, B. E. A. Saleh, and T. Khorsandi, "Theory of the temporal response of a simple multiquantum-well avalanche photodiode," *IEEE Trans. Electron. Dev.*, vol. 35, pp. 1456–1467, 1988.
[33] R. B. Emmons, "Avalanche-photodiode frequency response," *J. Appl. Phys.*, vol. 38, pp. 3705–3713, 1967.
[34] R. B. Emmons and G. Lucovsky, "The frequency response of avalanching photodiodes," *IEEE Trans. Electron. Dev.*, vol. ED-13, pp. 297–305, 1966.
[35] S. Riad and A. Riad, "Time-domain simulation analysis of avalanche photodetectors," *IEEE Trans. Electron. Dev.*, vol. ED-29, pp. 994–998, 1982.
[36] A. A. R. Riad and R. E. Hayes, "Simulation studies in both the frequency and time domains of InGaAsP avalanche photodetectors," *IEEE Trans. Electron. Dev.*, vol. ED-27, pp. 1000–1003, 1980.
[37] J. F. Chang, "Frequency response of pin avalanching photodiodes," *IEEE Trans. Electron. Dev.*, vol. ED-14, pp. 139–145, 1967.
[38] I. M. Naqvi, "Effects of time dependence of multiplication process on avalanche noise," *Solid-State Electron.*, vol. 16, pp. 19–28, 1973.
[39] A. A. Walma and R. Hackam, "On the time dependency of the avalanche process in semiconductors," *Solid State Electron.*, vol. 18, pp. 511–517, 1974.
[40] D. Snyder, *Random Point Processes.* New York: Wiley-Interscience, 1975.
[41] E. Parzen, *Stochastic Processes.* San Francisco: Holden-Day, 1962.
[42] J. Strikwerda, *Finite Difference Schemes and Partial Differential Equations.* California: Wadsworth and Brooks/Cole, 1989.

Gokalp Kahraman (S'90) was born in Izmir, Turkey. He received the B.S. degree from the University of Pennsylvania, Philadelphia, in 1986 and the M.S. degree from the University of Wisconsin, Madison, in 1988, both in electrical engineering. He is currently working toward the Ph.D. degree at the University of Wisconsin-Madison, Department of Electrical and Computer Engineering. His research interests include physics of electronic and optoelectronic devices, optical amplifiers, optical communications, and quantum optics.

Bahaa E. A. Saleh (M'73–SM'86–F'91) received the B.S. degree from Cairo University, Cairo, Egypt, in 1966 and the Ph.D. degree from the Johns Hopkins University, Baltimore, MD, in 1971, both in electrical engineering.

From 1971 to 1974 he was an Assistant Professor at the University of Santa Catarina, Brazil. Thereafter, he joined the Max Planck Institute in Gottingen, Germany. He is presently Professor and Chairman of the Department of Electrical and Computer Engineering at the University of Wisconsin, Madison, where he has been since 1977. He held visiting appointments at the University of California, Berkeley, in 1977, and the Columbia Radiation Laboratory of Columbia University in 1983. He is currently involved in research in statistical optics, optical communication, image processing, and vision. He is the author of *Photoelectron Statistics* (Springer, 1978), and coauthor of *Fundamentals of Photonics* (Wiley, 1991).

Dr. Saleh is a Fellow of the Optical Society of America and John Simon Guggenheim Foundation. He is currently the Editor of the *Journal of Optical Society of America A* and a member of the Editorial Board of *Quantum Optics.*

Malvin C. Teich (S'62–M'66–SM'72–F'89) was born in New York City. He received the S.B. degree in physics from the Massachusetts Institute of Technology, Cambridge, MA, in 1961, the M.S. degree in electrical engineering from Stanford University, CA, in 1962, and the Ph.D. degree in quantum electronics from Cornell University, Ithaca, NY, in 1966.

In 1966, he joined the MIT Lincoln Laboratory, Lexington, MA, where he was engaged in work on coherent infrared detection. In 1967, he became a member of the faculty in the Department of Electrical Engineering, Columbia University, NY, where he is now teaching and pursuing his research interests in the areas of quantum optics, optical and infrared detection, and sensory perception. He served as Chairman of the Department from 1978 to 1980. He is also a member of the faculty in the Department of Applied Physics, and a member of the Columbia Radiation Laboratory, the Center for Telecommunications Research, and the Fowler Memorial Laboratory at the Columbia College of Physicians & Surgeons. He has authored or coauthored some 150 technical publications and holds one patent. He is the coauthor, with B. Saleh, of *Fundamentals of Photonics* (Wiley, 1991).

Dr. Teich was the recipient of the IEEE Browder J. Thompson Memorial Price Award for his paper "Infrared Heterodyne Detection" in 1969, and in 1981 he received the Citation Classic Award of the Institute for Scientific Information for his work. He was awarded a Guggenheim Fellowship in 1973. He is a Fellow of the American Physical Society, the Optical Society of America, and the American Association for the Advancement of Science. He is a member of Sigma Xi, Tau Beta Pi, the Acoustical Society of America, the Association for Research in Otolaryngology, and the New York Academy of Sciences. He served as a member of the Editorial Advisory Panel for the journal *Optical Letters* from 1977 to 1979. He is currently Deputy Editor of the journal *Quantum Optics* and a Member of the Editorial Board of the *Journal of Visual Communication and Image Technology.*